treated hydroxyapatite, and fluoroapatite coatings on titanium. J Biomed Mater Res 1995;29:1053–1060.
3. Borts SA, Onesto EJ. Flame-sprayed bioceramics. Am Ceram Soc Bull 1975;52:898.
4. Kokubo T. Surface chemistry of bioactive glass-ceramics. J Non-Cryst Solids 1990;120:138–.
5. Weinlaender III MJB, Kenney EB, Moy PK. Raman microprobe investigation of the calcium phosphate phases of three commercially available plasma-flame-sprayed hydroxyapatite-coated dental implants. J Mater Sci Mater Med 1992;3:397–401.
6. Taguchi T, Kishida A, Akashi M. Hydroxyapatite formation on/in hydrogels using a novel alternate soaking process. Chem Lett 1998;8:711–712.
7. Taguchi T, Kishida A, Akashi M. Apatite formation on/in hydrogels using a novel alternate soaking process (II): Effect of swelling ratio on apatite formation on/in poly(vinyl alcohol) hydrogel matrix. J Biomater Sci Polym Ed 1999;3:331–339.
8. Taguchi T, Kishida A, Akashi M. Apatite formation on/in hydrogels using a novel alternate soaking process (III): Effect of physico-chemical factors on apatite formation on/in poly(vinyl alcohol) hydrogel matrix. J Biomater Sci Polym Ed 1999;10: 795–804.
9. Serizawa T, Kawanishi N, Akashi M. Hydroxyapatite deposition by alternating soaking technique on poly(vinyl alcohol)-coated polyethylene films. J Biomater Sci Polym Ed 2001;12: 1293–1301.
20. Tanahashi M, Yao T, Kokubo T, Minoda M, Miyamoto T, Nakamura T, Yamamuro T. Apatite coated on organic polymers by biomimetic process: improvement in its adhesion to substrated by NaOH treatment. J Appl Biomater 1994;5:339–347.
21. Margaret AH, Todd JA, Guyot-Sionnest P. Conformation of alkanethiols on Au, Ag(111), and Pt(111) electrodes: A vibrational spectroscopy study. Langmuir 1995;11:493–497.
22. Lindberg O, Ernster L. Determination of organic phosphorus compounds. Methods Biochem Anal 1956;3:1–22.
23. Connerty HV, Briggs AR. Determination of serum calcium by means of orthocresolphtalein complexone Am J Clin Pathol 1966;45:290–296.
24. Tanahashi M, Matsuda T. Surface functional group dependence on apatite formation on self-assembled monolayers in a simulated body fluid. J Biomed Mater Res 1997;34:305–315.
25. Tamatani S, Ogawa T, Minakawa T, Takeuchi S, Koike T, Tanaka R. Histological interaction of cultured endothelial cells and endovascular embolic materials coated with extracellular matrix. J Neurosurg 1997;86:109–112.
26. Mcguire PG, Orkin RW. Isolation of rat aortic endothelial cells by primary explant techniques and their phenotypic modulation by defined substrata. Lab Invest 1987;57:94–105.

Physical and Biological Evaluations of Sintered Hydroxyapatite/ Silicone Composite with Covalent Bonding for a Percutaneous Implant Material

Tsutomu Furuzono,[1] Pao-Li Wang,[2] Arata Korematsu,[1] Kozo Miyazaki,[1] Mari Oido-Mori,[3] Yusuke Kowashi,[3] Kiyoshi Ohura,[2] Junzo Tanaka,[4] Akio Kishida[1]

[1] Department of Bioengineering, National Cardiovascular Center Research Institute, 5-7-1 Fujishiro-dai, Suita, Osaka 565-8565, Japan

[2] Department of Pharmacology, Osaka Dental University, 8-1 Kuzuhahanazono-cho, Hirakata 573-1121, Japan

[3] Department of Periodontology and Endodontology, School of Dentistry, Health Sciences University of Hokkaido, 1757 Ishikari-Tobetsu, Hokkaido 061-0293, Japan

[4] Bioceramics Research Group, Independent Administrative Institution, National Institute for Materials Science, Advanced Materials Laboratory, 1-1 Namiki, Tsukuba, Ibaraki 305-0044, Japan

Received 21 March 2002; revised 3 September 2002; accepted 2 October 2002

Abstract: **A composite (HA/silicone) of hydroxyapatite (HA) microparticles with an average diameter of 2.0 μm covalently linked to a silicone substrate has been developed, and its physical and biological properties as a percutaneous soft-tissue-compatible material have been evaluated. In tensile property measurement, samples of HA/silicone and the original silicone were similar in tensile strength, ca. 7.8 MPa, and elongation at break, ca. 570%. It was found that chemical surface modification with HA particles presented no mechanical disadvantage. In an adhesive-tape peeling test, scanning electron microscopic (SEM) observation showed that HA particles coupled directly to the substrate were not removed. HA particles may bond strongly with the substrate. In human periodontal ligament fibroblast attachment and proliferation experiments, the number of cells attached to HA/silicone was 14 times greater than that attached to the original silicone after 24 h of incubation. The value on HA/silicone was ca. 80% versus that on a tissue-culture plastic used as a positive control. After 72 h of incubation, the number of cells grown on HA/silicone increased to the level of the positive control. In observation of fluorescence microscopy stained by Hoechst 33342, cells appeared to tightly adhere to HA particles coupled to the silicone sheet due to intact nuclear morphology. Observation of cells by fluorescence dye with rhodamin phalloidin showed an extensive F-actin cytoskeleton on HA/silicone. In a 4-week animal implant test, force required to pull out the HA/silicone sheet was 15 times that of the original silicone. HA-particle coating on silicone with covalent linkage gave the inert surface bioactivity. The HA composite thus effectively prevents germ infection percutaneously.** © 2003 Wiley Periodicals, Inc. J Biomed Mater Res Part B: Appl Biomater 65B: 217–226, 2003

Keywords: **hydroxyapatite; silicone elastomer; composite; covalent bonding; percutaneous implantation**

INTRODUCTION

Many artificial organs and devices, such as ventricular assist devices,[1] peritoneal dialysis catheters,[2] blood-access tubes,[3] and intragastric nutrition devices,[4] are implanted percutaneously *in vivo* through the skin. To ensure that such organs and devices can be used safely for long periods, infection must be prevented from occurring through such devices. Attempts have been made to develop organic,[5] inorganic,[6] and metallic materials[7] for 50 years. Silicone elastomer, a typical implantable material, has long been used in catheters. Infection occurs easily through silicone tubes inserted *in vivo*, and many approaches have been tried to retain percutaneous materials long term without epidermal downgrowth and infection, but with little success.

Correspondence to: T. Furuzono, Department of Bioengineering, National Cardiovascular Center Research Institute, 5-7-1, Fujishiro-dai, Suita, Osaka 565-8565, Japan (e-mail: furuzono@ri.ncvc.go.jp)

Contract grant sponsor: CREST of Japan Science and Technology Corporation (JST)

A typical example of an inorganic biomaterial, sintered hydroxyapatite (HA), shows good compatibility with soft tissue.[6] Its bioactivity favorably adsorbs adhesion molecules or growth factors *in vivo* on HA.[8,9] Aoki developed percutaneous material with the use of sintered HA clinically in catheters, blood pressure transducers, leads, and electrodes.[6] A rigid ceramic disc that partially protrudes through the skin like this may, however, limit mobility and cause discomfort. Zabetakis et al. demonstrated thin-film HA coated on a flexible silicone catheter by pulsed laser deposition.[10] Unfortunately, the amorphous HA coating induced slightly inflammatory response in the animal study and cracks in the coating resulted from bending, while this composite maintained flexibility.

A composite of sintered HA microparticles covalently coupled to a silicone elastomer was developed.[11] The HA layer was formed by covalently linking amino groups of modified HA particles and a silicone substrate grafted with a polymer containing carboxyl groups. This surface modification is expected to give HA bioactivity to the surface of an elastic implant without impairing substrate elasticity. The physical and biological evaluations of the composite for a percutaneous material consisting of covalently bonded HA particles and silicone elastomer are detailed here. Composite physical properties have been evaluated via tensile and peeling strength, and biological properties via cell-culture and animal studies.

MATERIALS AND METHODS

Materials

Silicone sheets (0.3 mm thick; Shin-Etsu Polymer Co., Tokyo, Japan) were purified with methanol with a soxhlet extractor for 24 h, rinsed in distilled water, and dried for 24 h in a vacuum at ambient temperature. Sintered, spherical, carbonated HA particles with an average diameter of 2.0 μm were kindly donated by Asahi Pentax Co., Ltd. (Tokyo, Japan).

Preparation of HA/Silicone Composite

The preparation of the HA/silicone composite is as reported elswhere.[11] Briefly, an acrylic acid-grafted silicone sheet was prepared by radical polymerization with corona-discharge treatment.[12] HA particles were subsequently modified with amino groups with the use of γ-aminopropyltriethoxysilane (γ-APS, Shin-Etsu Chemical Industries Co., Tokyo, Japan). Approximately one molecule per 300 Å^2 of amino-group density on the HA was used in all experiments. After formation of ammonium ionic bonds between samples under aqueous conditions, samples were reacted at 180 °C for 6 h in a vacuum at 1 mm Hg to form covalent bonds to the polyacrylic acid-grafted silicone (PAAc-*g*-silicone) surface by covalent linkage. The coverage ratio of HA particles was calculated to be approximately 65% (sd=6.3, n=3) by SEM observation.

Physical Properties

Tensile properties were measured with the use of a Tensilon RTC-115 OA (Orientic Co., Tokyo, Japan) at an elongation of 30 mm/min. Measurement was at room temperature with film samples 10 mm wide, 40 mm long, and 0.3 mm thick, and four determinations were averaged.

The qualitative bonding strength between HA particles and the silicone substrate was evaluated based on the method of Tretinnikov et al.[13] The silicone sheet coated covalently with HA particles was pressed onto adhesive tape (Scotch, Catalog No. 810-1-12) at 1 mm Hg for 10 s. The tape was removed and residual HA particles on the silicone substrate were analyzed by scanning-electron microscopy (SEM, JSM-6301F; JEOL, Tokyo, Japan) at 10 kV. Before being placed in the SEM chamber, samples were platinum coated to prevent charging.

Cell Culture

Human periodontal ligament fibroblast-like cells (HPLFs) from explants of human normal gingival tissue of a healthy permanent tooth surgically extracted for orthodontic reasons,[14] were cultured in complete α-minimum essential medium (α-MEM, Gibco Laboratories Inc.), supplemented with heat-inactivated 10% fetal bovine serum (FBS, Gibco), 50 IU/ml of penicillin, 50 μg/ml of streptomycin, and 2.5 μg/ml of amphotericin B (ICN Biomedicals Inc.). Cells were cultured at 37 °C in an atmosphere of 5% CO_2 in a humidified incubator.

To detect cell proliferation on sample substrates (HA/silicone, the original silicone, and 0.1% gelatin-coated glass), HPLFs on samples were counted with the use of a hemacytometer. HPLFs were plated onto 24-well multiplates at 1×10^5 cells/well in α-MEM with 10% FCS, and incubated at 37 °C for 24, 48, and 72 h. After a predetermined time, samples were washed three times in phosphate-buffered saline [PBS(-)]. After cells were collected by trypsinization and diluted with a trypan blue/α-MEM mixture after centrifugation, cells were counted with a hemacytometer. Cell morphology on incubated samples was observed by SEM. Samples for SEM observation were prepared as detailed below. After being rinsed with PBS(-), sample films were fixed with 2.5% buffered-glutaraldehyde for 20 min at 30 °C. Cells were dehydrated with aqueous ethanol (30–100%) and 100% n-butanol for 5 min at room temperature step by step. Samples were lyophilized and coated with platinum.

Nuclear morphology of HPLFs on samples incubated 72 h was double-stained by Hoechst 33342 (1 μM, Calbiochem®, Tokyo, Japan) and propidium iodide (50 μg/ml, PI, Sigma Chemical Co., St. Louis, MO), and observed by fluorescence microscopy. F-actin of cells adhering to samples for 24 and 72 h were stained by rhodamin phalloidin (Wako Pure Chemical Industries, Ltd., Osaka, Japan) and observed by Bio-Rad MRC-1024 confocal laser-scanning microscopy.

ANIMAL STUDY

Animals were treated based on the Guideline for Animal Experimentation National Cardiovascular Center. Female Wister rats (Japan SLC, Inc., Shizuoka, Japan) weighing 150 g were anesthetized with ethyl ether. Their backs were shaved and incised about 1.5 cm, 5.0 cm deep. Sample films (1.0 × 5.0 cm) sterilized by an autoclave were per- or subcutaneous implanted where an incision was made; 20 mg/kg of piperacillin sodium (Sankyo Pharmaceutical Co., Tokyo, Japan), an antibacterial drag, was intraperitoneally administered once after implantation, and neither clearing of the implanted site nor further administration was made throughout implantation.

Three *in vivo* experiments—a percutaneous implantation test, histological observation, and a pull-out measurement with a subcutaneous implant material—were made individually. In the percutaneous implantation test, the appearance of implanted percutaneous sample sheets was recorded by a digital camera (Cool PIX 990, Nikon, Inc., Tokyo, Japan) after 6 days of implantation. Histological observation was conducted after subcutaneous implantation into the backs of rats. After 2 weeks of implantation, rats were sacrificed and the back was dissected to expose implanted samples. Sheets containing tissue were fixed with 10% buffered formalin, and sectioned with a microtome. Thin sectioned samples were stained with hematoxylin-eosin and examined under light microscopy. Pull-out measurement was done after 4 weeks of implantation. After rats were sacrificed, the back was dissected to expose subcutaneous implanted sample sheets. After careful exposure of the end of implanted samples from surrounding tissue, the exposed end was clamped with a clip connected to a tensile tester equipped with a 49-N load cell, and pull-out was measured moving upward at the rate 30 mm/min.

Statistical Analysis

Data resulting from the tensile test of the composite, the cell counting, and the pull-out measurement of subcutaneous implant are presented as means ± standard deviation for mean. Statistical comparisons were preformed with the use of a student's t test, and p values < 0.005 were considered statistically significant.

RESULTS

Physical Properties

Tensile properties, that is, tensile strength, elongation at break, and Young's modulus, were measured with the use of a silicone sheet coated with sintered HA microparticles by covalent bonding. Figure 1 shows tensile properties of the original silicone and HA/silicone composite sheet. Tensile strength and elongation at break of both samples showed the same value statistically, ca. 7.7 MPa and ca. 570%. The

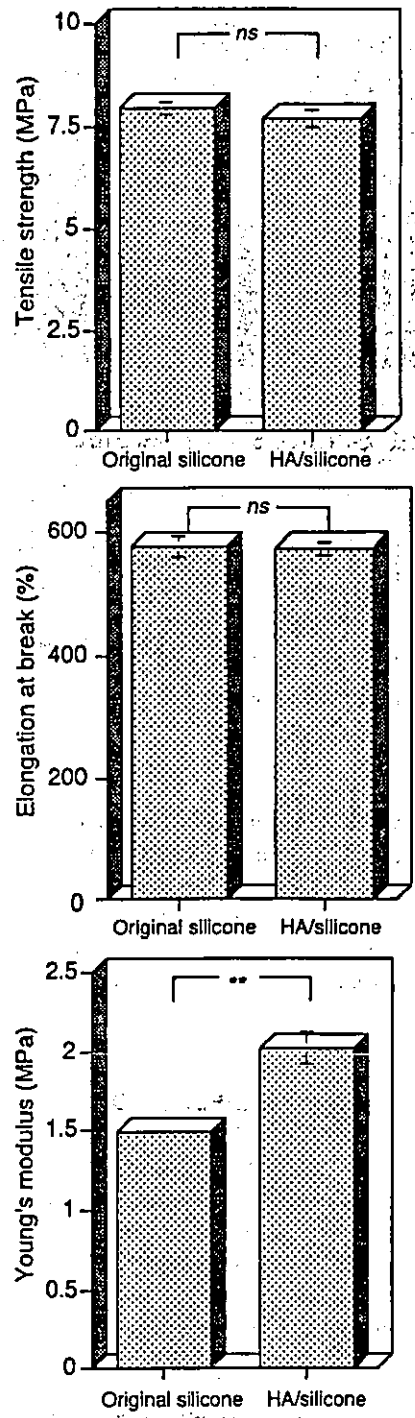

Figure 1. Tensile properties of HA/silicone and original silicone sheets. Data were calculated as means of quadruplicate determinations. Error bars represent standard deviation of quadruplicates (**$p <$ 0.005).

Young's modulus of HA/silicone was 1.3 times higher than that of the original. Figure 2 shows original and HA modified sample sheets. HA/silicone sheets turned from transparent to white by HA coating [Figure 2(b)]. The composite was very flexible and easily formed maintaining elastomer mechanical properties [Figure 2(a)].

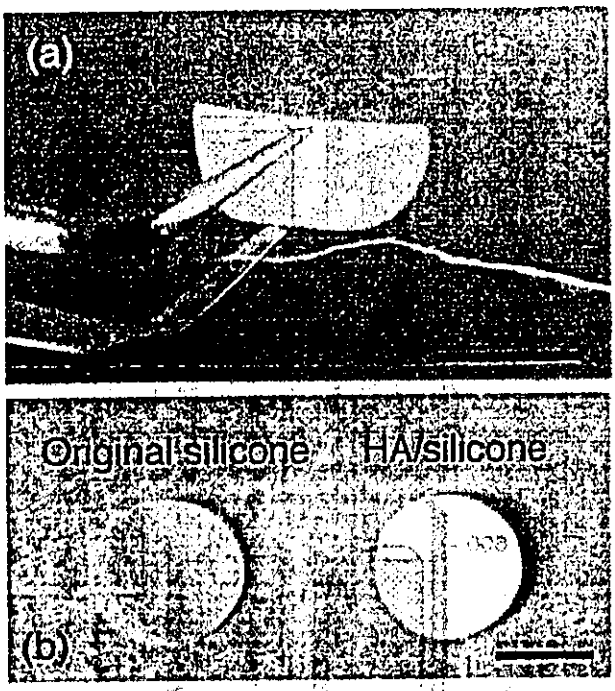

Figure 2. External view of HA/silicone and original silicone sheets. Bars indicate 10 mm.

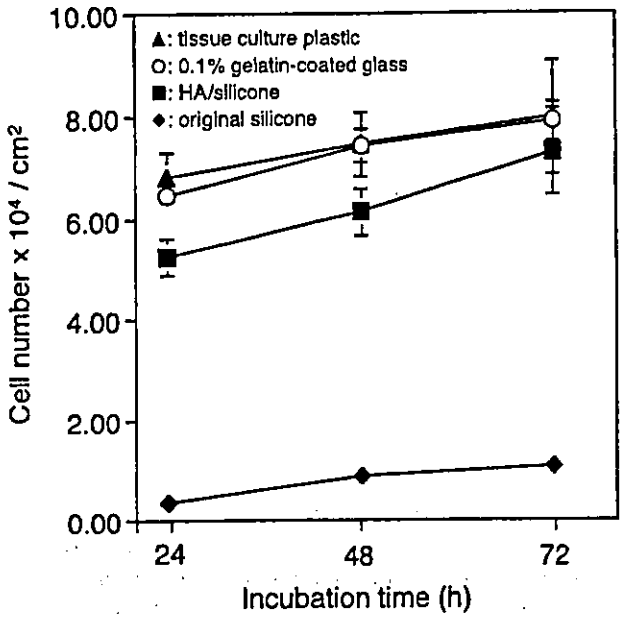

Figure 4. HPLF proliferation cultured on four culture substrates: HA/silicone; (b), the original silicone; (f), tissue-culture plastic; (h), and 0.1% gelatin-coated glass; (e), in 24-well multiplates at 1 × 10^5 cells/well, and incubated for at 37 °C for 72 h. Data were calculated as means of quadruplicate determinations. Error bars represent standard deviation of quadruplicates.

Figure 3 shows SEM before and after the peeling test as a qualitative evaluation of bonding strength between HA particles and the silicone surface. SEM observation showed HA particles linked to the substrate were not removed by peeling using adhesive tape. It was also found that overlapped particles separated partially from those attached directly to silicone.

CELL PROLIFERATION

HPLF density of about 57,000 cells/cm^2 was scattered on several substrates, such as HA/silicone, the original silicone, tissue culture plastic, and the 0.1% gelatin-coated cover glass. Figure 4 shows cell proliferation curves on samples after 24, 48, and 72 h of incubation. The number of cells adhering to HA/silicone substrate for 24 h of incubation was 14 times higher than that on the original silicone substrate, although that of HA/silicone was about 80% versus that on tissue-culture plastic. After 72 h of incubation, cells grown on HA/silicone substrate reached a statistically similar level to those of the positive control, although lower on the original silicone at each of the three time points.

HPLF morphology on three sample substrates incubated for 24, 48, and 72 h was observed by SEM (Figure 5). Glass was used as a positive control showing similar cell growth on tissue-culture plastic (Figure 4). Observing HPLF morphology on HA/silicone, cells adhered independently to the substrate separated after 24 h of incubation, although few were found on the original silicone surface. Cells proliferated and adhered to HA/silicone at over 48 h of incubation. The cell-matrix was fully covered after 72 h of incubation. Ex-

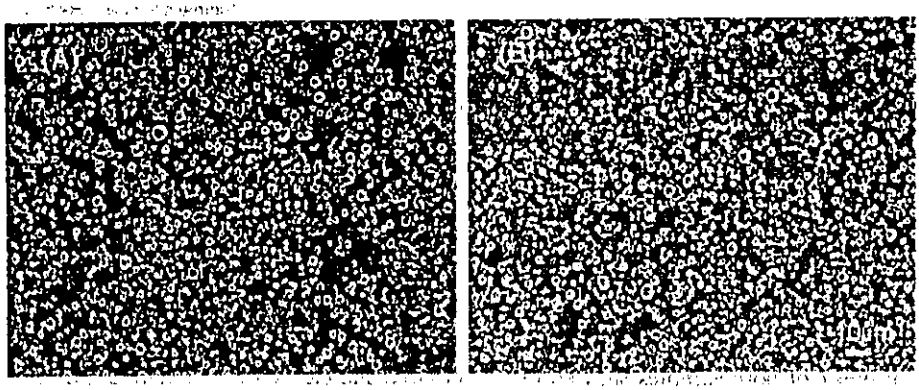

Figure 3. SEM images of HA/silicone surfaces (a) before and (b) after peeling with adhesive tape.

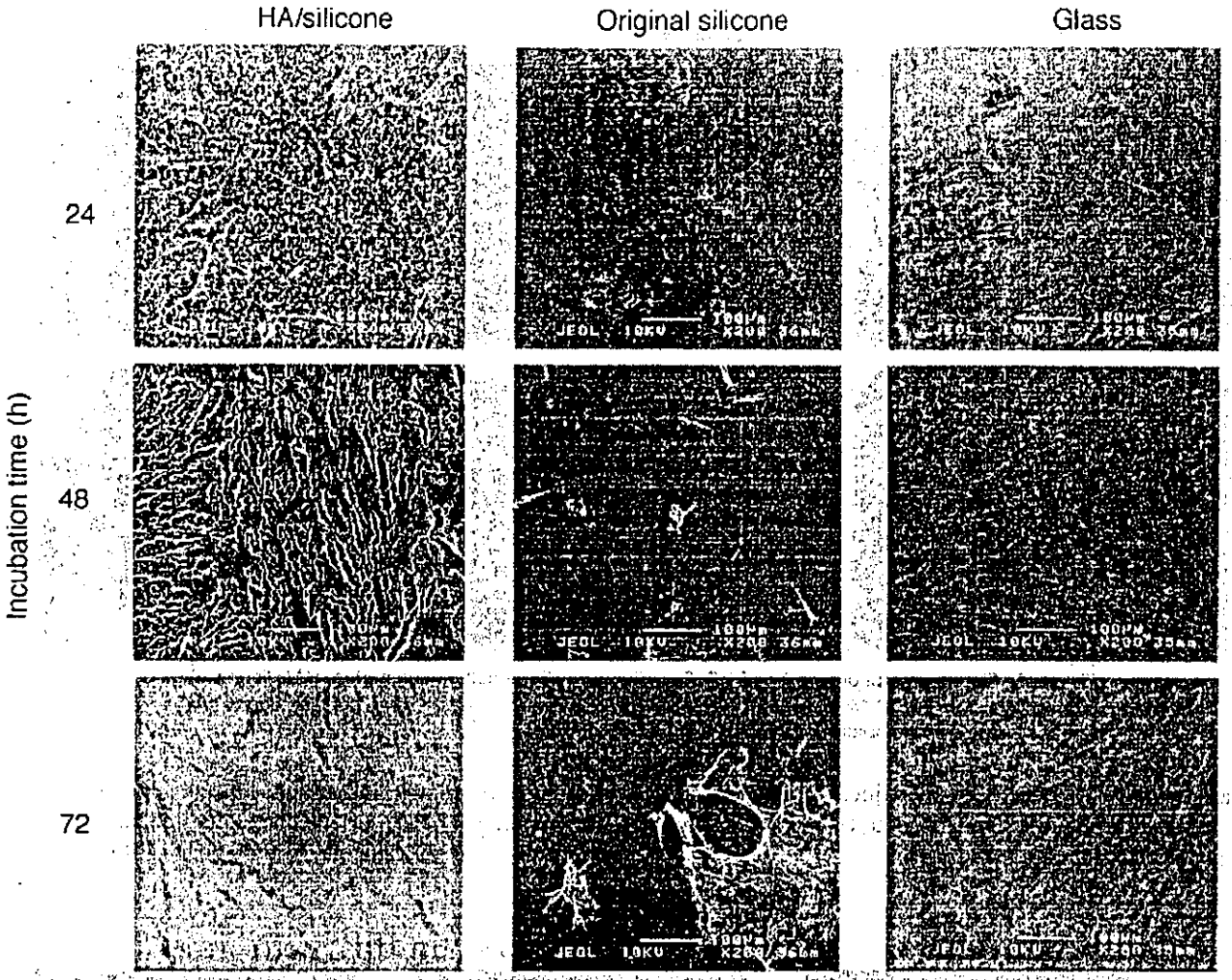

Figure 5. SEM images of HPLFs cultured on three culture substrates: HA/silicone, the original silicone, and 0.1% gelatin-coated glass, for 24, 48, and 72 h.

traordinary grown cells were observed partially on the original silicone surface.

Figure 6 shows nuclei of HPLFs stained by two fluorescence dyes on sample substrates after 72 h of incubation. Upper and lower photographs are observed at high and low magnification, respectively. Red cells stained with PI are dead. It was found that the matrix membrane consisting of living cells fully covered the HA/silicone substrate at 72 h of incubation, although cells scattered and partially grew with aggregation, including dead ones on the silicone substrate. This is usually observed as cell morphology adhered and grew on a more hydrophobic surface.[15] It was found that cells adhered to HA/silicone as a monolayer as well as glass, the positive-control substrate, because nuclei separated in fluorescence photographs. Figure 7 shows confocal microscopy of phodamin phalloidin-stained F actin of cells on sample substrates. On HA/silicone and glass, stained F actin showed HPLFs adhered and grew on surfaces. Incubating over 48 h showed a more extensive F actin cytoskeleton, with some spreading on HA/silicone. Actin filament did not extend to original silicone even at 72 h of incubation.

Animal Test

HA/silicone and original silicone sheets were implanted percutaneously into the backs of rats for 6 days. Percutaneous implantation could not be conducted for longer than 2 weeks because rats pulled out test samples, especially the original silicone sheet, implanted percutaneously. In the percutaneous animal implant test, skin tissue adhered strongly to HA/silicone and the wound healed dramatically after only 6 days of implantation (Figure 8), although tissue did not adhere to the original silicone surface undergoing inflammation.

The interface between the host and foreign body in the subcutaneous implantation test for 2 weeks was observed histologically (Figure 9). In the sectional view of the HA/silicone sheet, the edge of the sheet remained along the interface of tissue observed in the photographs, whereas the center of the sample implanted was removed by cutting with a microtome. There are some lymphocytes, fibroblasts, and thin fibrous tissue oriented parallel to the material surface by hematoxylin-eosin stain. Especially, it can be assumed that HA particles remain in the stained area on the material

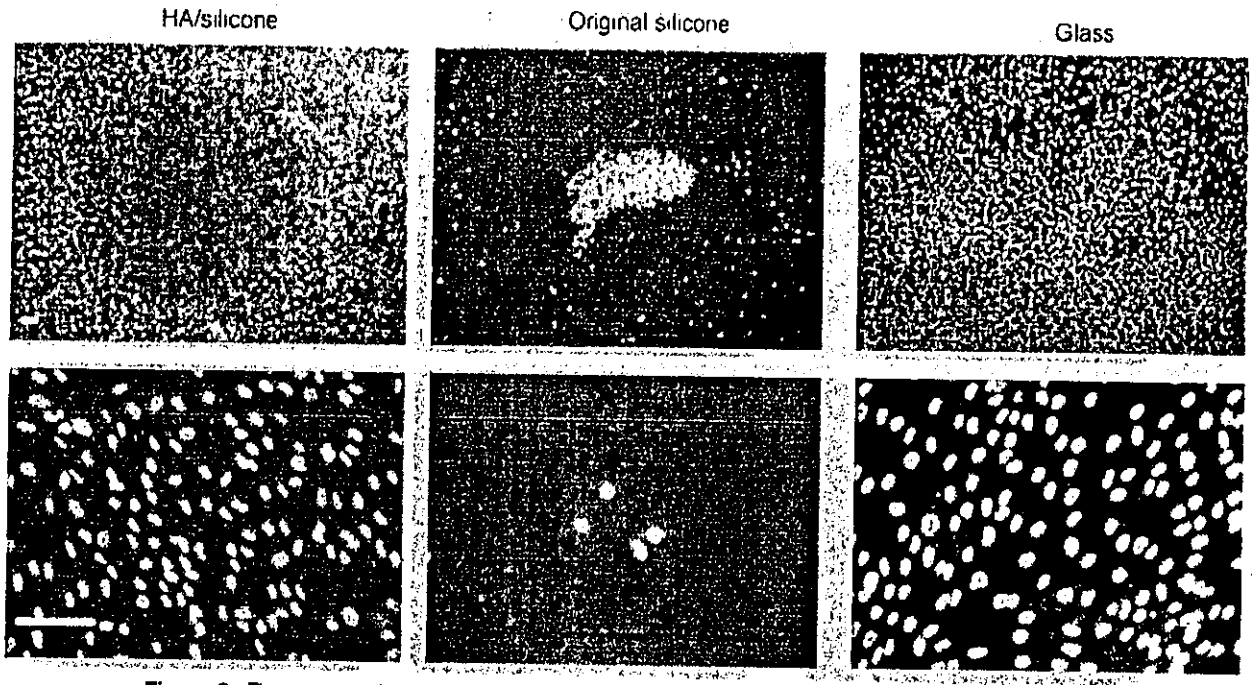

Figure 6. Fluorescent photographs of HPLFs cultured on three culture substrates: HA/silicone, the original silicone, and 0.1% gelatin-coated glass, for 72 h. Cell nuclei were double-stained with Hoechst 33342 and propidium iodide. Bars indicate 100 μm.

interface estimates. Under high magnification, surrounding tissue appeared to adhere more closely to HA/silicone than to the original silicone.

Figure 10 shows pull out of HA/silicone and original silicone after 4 weeks of subcutaneous implantation. Maximum pull out of HA/silicone from the backs of rats was 0.49

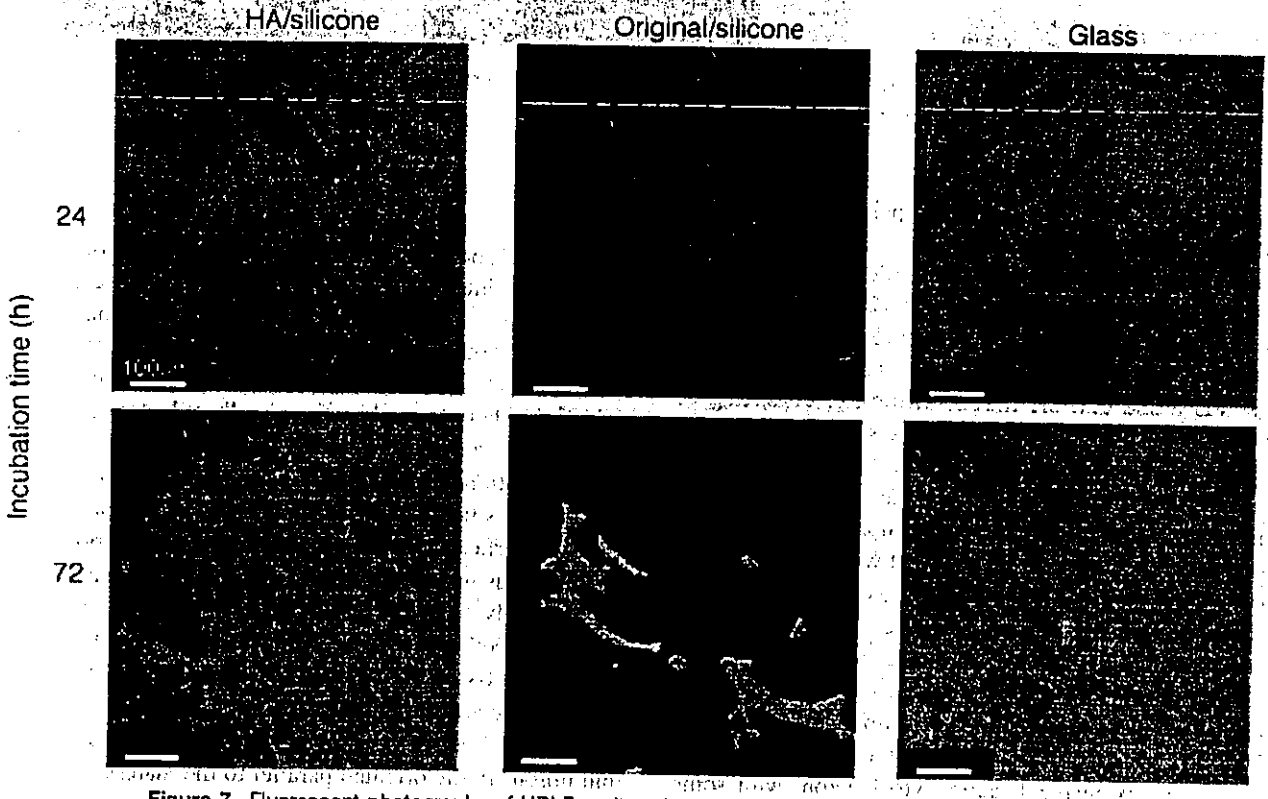

Figure 7. Fluorescent photographs of HPLFs cultured on three culture substrates: HA/silicone, the original silicone, and 0.1% gelatin-coated glass, for 24 and 72 h. Cells were stained with rhodamin phalloidin.

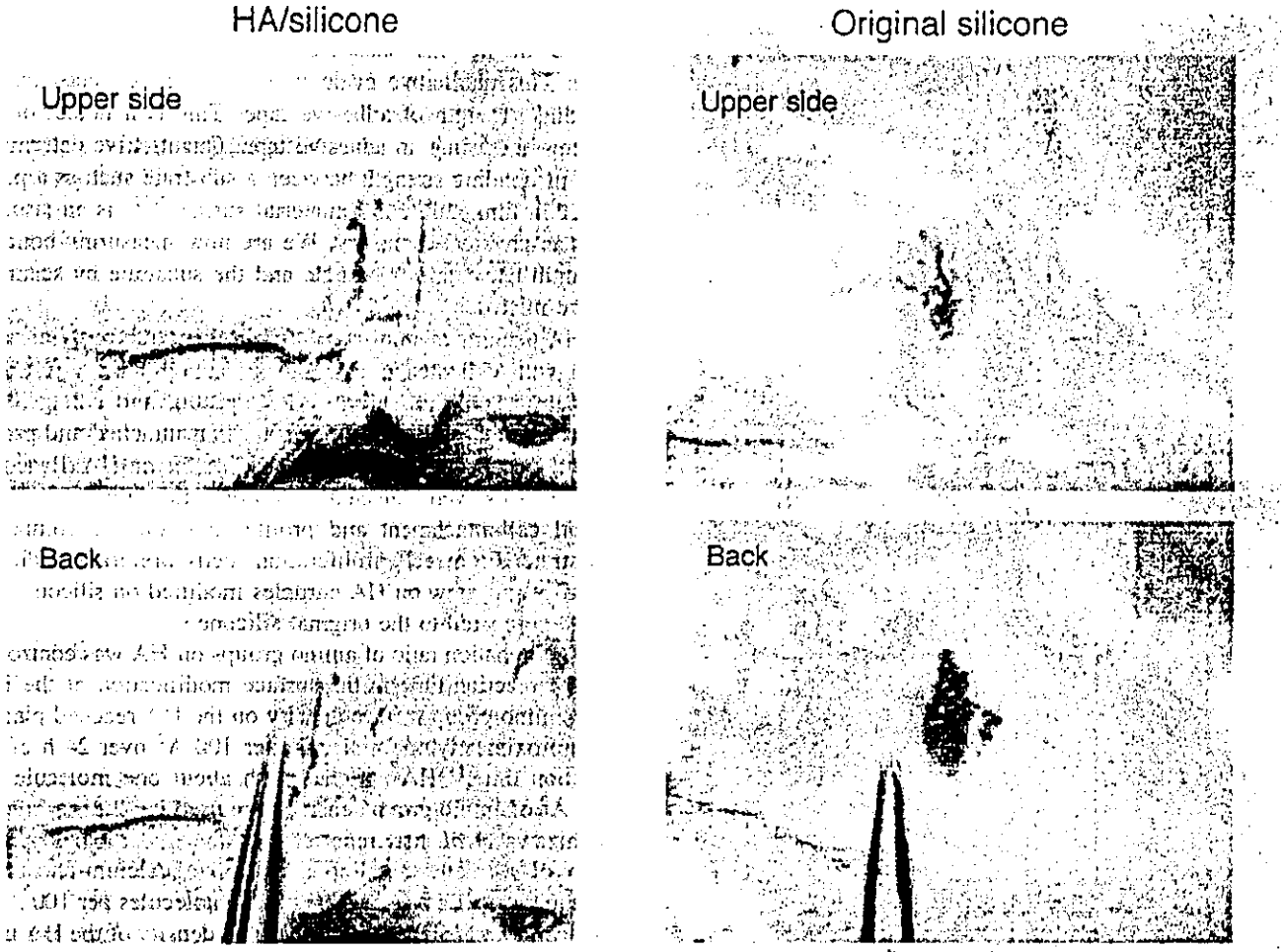

Figure 8. HA/silicone (left) and original silicone sheets (right) percutaneously implanted into the backs of rats.

N, while that of the original silicone was 0.03 N. The force of HA/silicone was thus about 15 times higher than that of the original silicone.

DISCUSSION

Several fabrication processes for HA and polymer composites have been reported, including biomimetic process,[16] plasma spraying,[17] coprecipitation method,[18] and alternate soaking process.[19] HA layers processed in these way easily dissolve *in vivo* due to low crystallinity. To maintain both bioactivity and biostability for a long period for a HA/polymer composite, it is necessary to chemically modify a substrate with sintered HA crystalline. Because the HA/silicone composite is prepared by surface coating on the silicone substrate with sintered HA microparticles by covalent linkage, it is expected that properties of both inorganic and organic materials can be expressed simultaneously. The existence of covalent linkage between amino-group donated HA and PAAc-*g*-silicone already has been estimated by an indirect method in an earlier report.[11] First, the condition of preparation of the composite such as reaction temperature and time was determined according to the synthetic method of the solid-phase polymerization of nylon. Next, the comparison of the FTIR spectra between PAAc-*co*-γ-APS and a heating product of PAAc-*co*-amino-groups donated HA was estimated the existence of covalent bonding.

Main tensile properties of the composite, such as tensile strength and elongation at break, were unchanged before and after surface modification with HA particles, except for Young's modulus (Figure 2). The Young's modulus of HA/silicone was somewhat higher statistically than that of the original, perhaps because the difference of the modulus may depend on ionic interaction among HA particles linked on the substrate. Because of the thin layer of inorganic substrate covering the surface of the silicone, HA/silicone was a little harder than the original one. The HA/silicone sheet remained flexible, showing the nature of an elastomer (Figure 2). The surface modification method via silicone elastomer was done in three steps—corona discharge treatment with input of 200 W, graft polymerization at 60 °C for 1 h, and heating at 180 °C for 6 h in a vacuum (1 mm Hg). Although these reactions were severe for widely used polymers such as polyethylene,

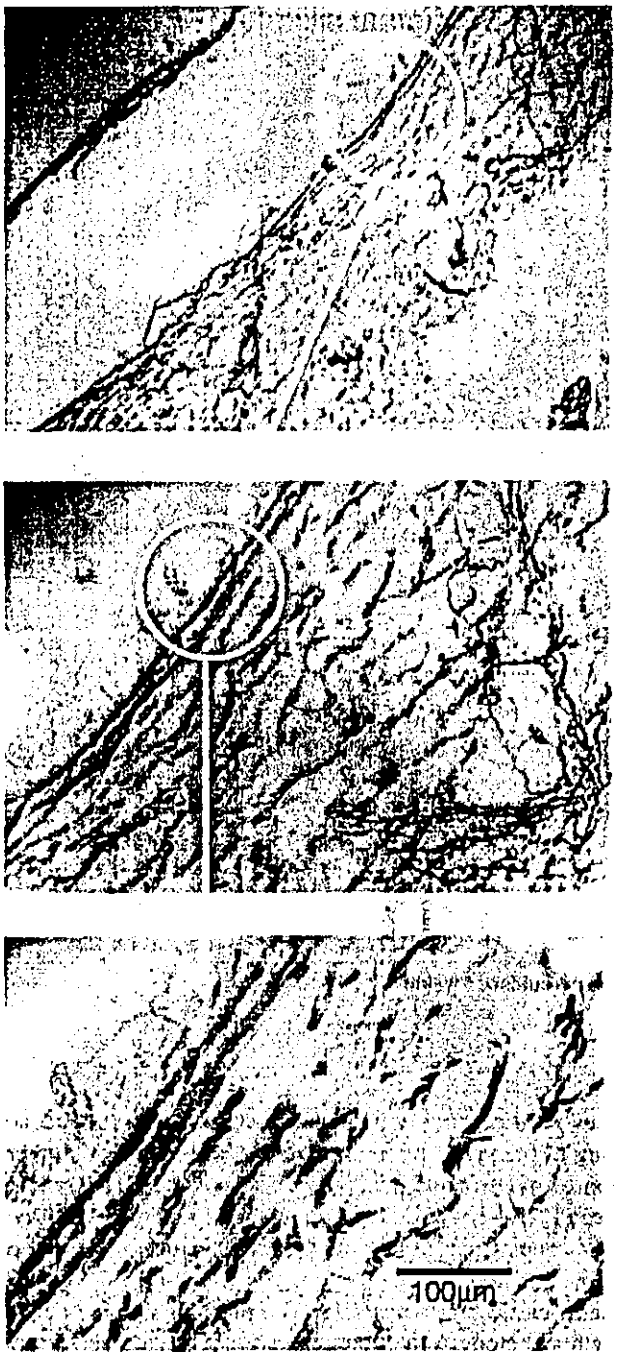

Figure 9. Histological appearance of HA/silicone implanted into the back of a rat for 14 days.

nylon, and polyurethane, the composite with silicone elastomer withstood such conditions due to its thermo-resistivity.

To determine qualitative bonding strength between HA particles and the substrate, we conducted a peeling test with the use of adhesive tape. Partially overlapped HA particles were removed from directly coupled to the substrate by peeling. This showed that HA particles strongly linked with the silicone surface by covalent bonding than HA particles attached to each other. Particles bonded directly onto the surface may not be removed under experimental conditions, that is, bonding strength between HA particles and the surface of the polymer substrate withstood peeling by adhesive tape. This qualitative evaluation, however, depends on the bonding strength of adhesive tape. This is a defect of the peeling test using an adhesive tape. Quantitative determination of bonding strength between a substrate such as a particle, thin film, cell, and a material surface[20,21] is an issue in surface physical chemistry. We are now measuring bonding strength between HA particle and the substrate by scanning probe microscopy.

HA, a component of cementum in the tooth root, interacts well with cell attachment, and spreading factors (CASFs) such as fibronectin, vitronectin, laminin, and collagen are released from HPLFs.[22] HPLFs are thus attached and proliferated through initial adsorption of CASFs on HA. Based on this, HPLFs were selected as fibroblastic cells to evaluate initial cell-attachment and proliferation on the composite substrate. From cell proliferation, cells preferably adhered initially and grew on HA particles modified on silicone substrate compared to the original silicone.

The donation ratio of amino groups on HA was controlled by the reaction time in the surface modification of the HA. The amino-group surface density on the HA reached plateau at approximately one molecule per 100 $Å^2$ over 24 h of the reaction time.[11] HA particles with about one molecule per 300 $Å^2$ of amino-group density were used in all experiments. Nishizawa *et al.* first reported that the maximum donation ratio of a silane coupling agent on a calcium-phosphate ceramic was calculated at three–four molecules per 100 $Å^2$.[23] This value was higher than that of the density of the HA used here. Therefore it was estimated that the HA surface used here had not only an amino-group donated surface but also

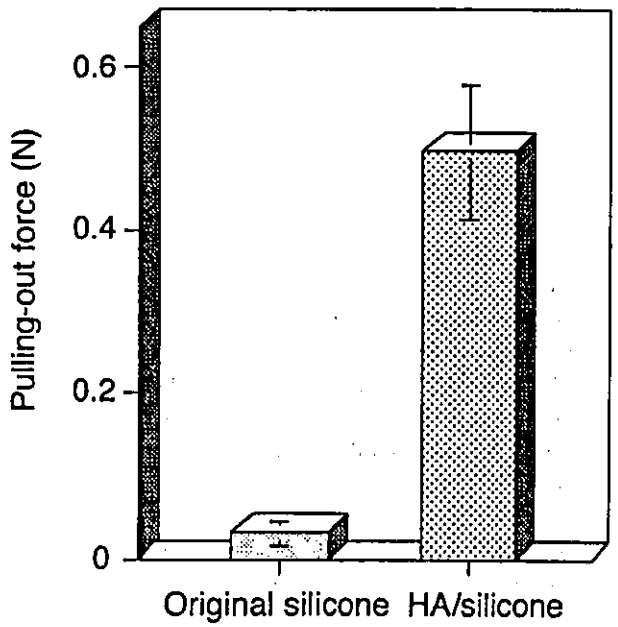

Figure 10. Maximum pull-out force of HA/silicone and original silicone sheets implanted into the backs of rats. Data were calculated as means of triplicate determinations (**$p < 0.005$).

the intact HA surface. Cationic groups promote initial cell adhesion and growth.[24] Amino groups in addition to the intact HA surface may influence initial cell adhesion and growth on HA/silicone. The cell-growth curve for HA/silicone was delayed compared to that of cell culture plastic, the positive control, and finally reached the same level statistically for 72 h. Craig and LeGeros reported levels of HPLF proliferation, and collagen and noncollagen protein synthesis for cells grown on the HA-coated surface lagged behind cells cultured on the cell-culture plate.[25] This may be because biomaterial substrates depend on the temporal sequence of extracellular matrix proteins associated with periodontal connective tissue attachment, and surface properties such as topography.

Compared to the matrix membrane on glass for 72 h of incubation in SEM, the matrix on HA/silicone looked thicker (Figure 5). In fluorescent photographs of nuclei double stained with both Hoechst 33342 and propidium iodide (Figure 6), it was clear that the matrix consisting of living cells showed a monolayer. In fluorescent photographs of HPLFs on samples stained with rhodamin phalloidin for 72 h of incubation (Figure 7), F actin spread on HA/silicone showed somewhat wider filament than that on glass. From this, it was assumed that cells adhered and expanded strongly on a HA particle to neighbors, making a bridge structure.

The percutaneous implantation test for 6 days was conducted to evaluate soft-tissue response to HA/silicone surface (Figure 8). The adhesion between skin tissue and sample surfaces depended on the physical, chemical, and topographic structures of the surface. Skin tissue adhered thoroughly and strongly to HA/silicone sheets, but not on the original silicone. The result of the experiment is easy to determine from data on the cell-incubation experiment. It is very important clinically that infection be blocked early on *in vivo* injury such as that due to a surgery in biomaterial implantation. It was concluded that a percutaneous device coated with HA particles with this surface modification may be effective for protecting against initial infection.

Histological observation after 2 weeks of implantation showed interaction between the surface of HA/silicone and soft tissue *in vivo* (Figure 9). The original silicone sheet in soft tissue could not be cut by a microtome because of differences in physical properties, such as elasticity and toughness, between the material and living tissue. Original silicone is easily excluded *in vivo* because of thick fibrous tissue oriented parallel to the original material surface.[26] An HA/silicone sheet surrounded with soft tissue could be cut with difficulty due to favorable adhesion of soft tissue on HA particles coupled to the silicone sheet. Surrounding tissue was attached strongly to HA/silicone sheet in histological appearance. A thin fibrous surrounding tissue over the HA/silicone sample in addition to tissue attachment closely supported the technical facts of sample cutting by a microtome as described above.

In pull out of sample sheets pulled from the backs of rats, the maximum force of HA/silicone sample was about 15 times higher than that of the original (Figure 10). Maximum pull-out force of collagen immobilized on a silicone sheet was about 12 times higher than that of the original after 3 weeks of implantation.[27] The 15- times-higher pull-out force of HA/silicone was slightly higher than that of the collagen-immobilized sample, possibly because of an anchoring effect between the soft tissue and HA particles coupled to the silicone substrate in addition to the effect of initial adsorption of CASFs, such as collagen, on the HA surface.

CONCLUSIONS

Physical and biological properties of a composite, silicone elastomer with sintered HA particles having an average diameter of 2.0 μm coupled by covalent linkage were evaluated for use in percutaneous implantation. The tensile test showed that the composite remained soft and flexible as an elastomer after surface modification with the HA microparticles. Biological tests through HPLF proliferation and composite-sheet implantation per- or subcutaneously in rat showed that HA/silicone improved adhesion via living tissue compared to the original. The HA coating on a medically implantable device thus effectively adds bioactivity to the surface. The composite in this study could be developed into elastic percutaneous devices in a variety of medical fields.

The authors thank Professor K. Ishihara, University of Tokyo, for aid in obtaining HA particles.

REFERENCES

1. Unger F. Assisted circulation 2. New York: Springer; 1984.
2. Thodis E. Passadakis P, Vargemezis V, Oreopoulos DG. Prevention of catheter related infections in patients on CAPD. Int J Artif Organs 2001;24:671–682.
3. Wildberger J. Schmitz-Rode T. Wein BB. Gunther RW. Mechanical thrombectomy in hemodialysis access shunt using a 5F pigtail rotation catheter. *In vitro* and *in vivo* investigations. Invest Radiol 1999;34:489–495.
4. Vega JD. Poindexter SM. Radovancevic B. Burnett CM. Lonquist JL. Birovljev S. Duncan JM. Frazier OH. Nutritional assessment of patients with extended left ventricular assist device support. ASAIO Trans 1990;36:M555–M558.
5. Pourchez T. Moriniere P. Fournier A. Pietri J. Use of permcath (quinton) catheter in uraemic patients in whom the creation of conventional vascular access for haemodialysis is difficult. Nephron 1989;53:297–302.
6. Aoki H. Medical applications of hydroxyapatite. Tokyo: Ishiyaku EuroAmerica Inc.; 1994.
7. Kawamura A. Yonekawa M. Kukita K. Meguro J. Tamaki T. Tanaka M. Horie T. Masuko Y. Iida J. Uchida Y. Murai N. Kaizu T. Arikura J. Abe H. No-needle blood access device for hemodialysis and no-needle connecting cannula assembly (K-NOBA PAT./JAP2983540).
8. Pitaru S. Savion N. Hekmati H. Olsen S. Narayanan SA. Binding of a cementum attachment protein to extracellular matrix components and to dental surfaces. J Periodontal Res 1992;27: 640–646.
9. Midy V. Rey C. Bres E. Dard M. Basic fibroblast growth factor adsorption and release properties of calcium phosphate. J Biomed Mater Res 1998;41:405–411.

10. Zabetakis PM, Cotell CM, Chrisey DB, Auyeung RC. Pulsed laser deposition of thin film hydroxyapatite. ASAIO J 1994;40: M896–M899.
11. Furuzono T, Sonoda K, Tanaka J. A hydroxyapatite coating covalently linked onto a silicone implant material. J Biomed Mater Res 2001;56:9–12.
12. Okada T, Ikada Y. Modification of silicone surface by graft polymerization of acrylamide with corona discharge. Makromol Chem 1991;192:1705–1713.
13. Tretinnikov ON, Kato K, Ikada Y. *In vitro* hydroxyapatite deposition onto a film surface-grafted with organophosphate polymer. J Biomed Mater Res 1994;28:1365–1373.
14. Somerman MJ, Young MF, Foster RA, Moehring JM, Imm G, Sauk JJ. Characteristics of human periodontal ligament cells *in vitro*. Arch Oral Biol 1990;35:241–247.
15. Tamada Y, Ikada Y. Fibroblast growth on polymer surfaces and biosynthesis of collagen. J Biomed Mater Res 1994;28:783–789.
16. Kokubo T, Kushitani H, Ohtsuki C, Sakka S, Yamamoto T. Chemical reaction of bioactive glass and glass-ceramics with a simulated body fluid. J Mater Sci Mater Med 1992;1:79-83.
17. de Groot K, Geesink R, Klein CPAT, Serekian P. Plasma sprayed coating of hydroxyapatite. J Biomed Mater Res 1987; 21:1375–1381.
18. Tanaka J, Cho SB. Development of organic–inorganic composite artificial bone based on self-organization phenomenon. J Oromax Biomech 1996;2:14–19.
19. Taguchi T, Kishida A, Akashi M. Hydroxyapatite formation on/in hydrogels using a novel alternate soaking process (I). Chem Lett 1998;8:711–712.
20. Yamamoto A, Mishima S, Maruyama N, Sumita M. Quantitative evaluation of cell attachment to glass, polystyrene, and fibronectin- or collagen-coated polystyrene by measurement of cell adhesive shear force and cell detachment energy. J Biomed Mater Res 2000;50:114–124.
21. Fujihira M, Aoki D, Okabe Y, Takano H, Hokari, H. Effect of force microscopy: A scanning hydrophilicity microscope. Chem Lett 1996;7:499–500.
22. Amino S, Kawase T. Cell attachment and spreading factors of human periodontal ligament fibroblasts. Bull Kanagawa Dent Col 1992;27:179–192.
23. Nishizawa K, Toriyama M, Suzuki T, Kawamoto Y, Yokogawa Y, Nagata F. Surface modification of calcium phosphate ceramics with silane coupling reagents. Chem Soc Jpn 1995;1:63–67.
24. Rosen JJ, Gibbons DF, Culp LA. Hydrogels for medical and related applications. In: Andrade JD, editor, ACS Symposium Series 31. Washington, DC: American Chemical Society; 1976. pp 329–343.
25. Craig RG, LeGeros RZ. Early events associated with periodontal connective tissue attachment formation on titanium and hydroxyapatite surfaces. J Biomed Mater Res 1999; 47: 585-594.
26. Furuzono T, Kishida A, Yanagi M, Matsumoto T, Kanda T, Nakamura T, Aiko T, Maruyama I, Akashi M. Novel functional polymers: Poly(dimethylsiloxane)-polyamide multiblock copolymer V. The interaction between biomolecules and the surface of aramid–silicone resins. J Biomater Sci Polym Ed 1996;7: 871–880.
27. Okada T, Ikada Y. Surface modification of silicone percutanous implantation. J Biomater Sci Polymer Ed 1995;7:171–180.

4. ESCAの測定法と接着

岸 田 晶 夫*

はじめに

ESCA (Electron Spectroscopy for Chemical Analysis) はX線光電子分光法 (X-ray Photoelectron Spectroscopy : XPS) の別名であり，軟X線を励起源とする分光法である。ESCA は最外層表面の元素分析法として広い分野で高い評価を得ており，接着分野においても有用な分析法である。ESCA については優れた成書・総説があるので[1~8]，ここではESCAの基本と接着現象解析への応用について解説する。

4.1 ESCAの測定原理

原子の核電子はそれぞれの軌道に特徴的な結合エネルギーによって束縛されている。ESCA は試料表面から放出された電子の結合エネルギーを測定しスペクトル化する。図 4.1 に示すように，軟X線が試料表面に照射されると，X線は高分子で約 1 μm 程度（金属・無機材料ではそれ以下）材料を透過し，材料を構成する原子の電子を励起する。励起された電子は材料中を通り抜けて表面から外に飛び出してゆく。外に飛び出した電子はそれぞれ源泉の原子固有のエネルギーを有している。この電子をエネルギー分散型の検出器で，あるエネルギーで飛来する電子だけをカウントする。一定時間ごとに電子数をカウントし，測定するエネルギー値を変化させてスペクトルを描いてゆく。H, He を除いて個々の元素から放出される電子のエネルギーについては一覧表があるので，スペクトルのピーク位置付近のエネルギー値がわかれば試料中の元素の存在が容易に判別できる。電子が外に飛び出せる深さには限界があり（表面から 100 オングストローム程度といわれている），これによって分析対象となる表面からの深さが規定されるため，ESCA は極表面分析が可能になっている。

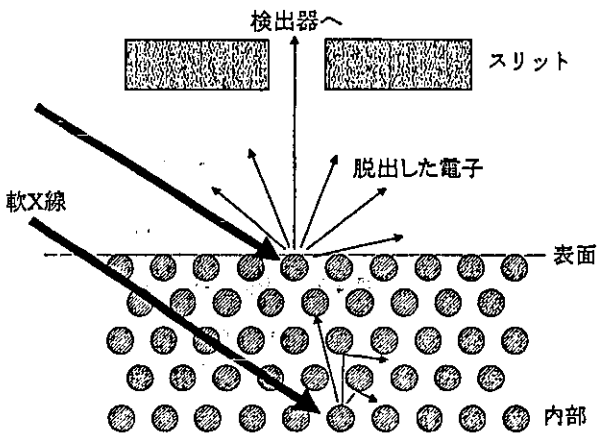

図 4.1 XPS の原理図

4.2 ESCAスペクトルの見方の例

図 4.2 に典型的な ESCA スペクトルを示す。図には横軸に「Binding Energy (eV)」，縦軸に「cps」とプロットされている。横軸は結合エネルギーで単位は eV，縦軸は count per second の略で，1 秒間あたりの検出電子数を意味する。横軸は増減の順が普通と逆になっている。使用する装置によっては正順（左が小さく右が大）のチャートを描くものもあるが，多くの場合，図 4.2 のように右にいくほど結合エネルギーが小さくなるように描画する。これは測定する電子の結合エネルギーと検出器で測定される光電子の運動エネルギーの符号が逆であることに由来すると思われる。図 4.2 の場合，2 つのピークが存在し，そのすそ野が少し重なっている。このスペクトル図から以下の事項を読みとることができる。

* 国立循環器病センター研究所 生体工学部
大阪府吹田市藤白台 5-7-1 〒565-8565

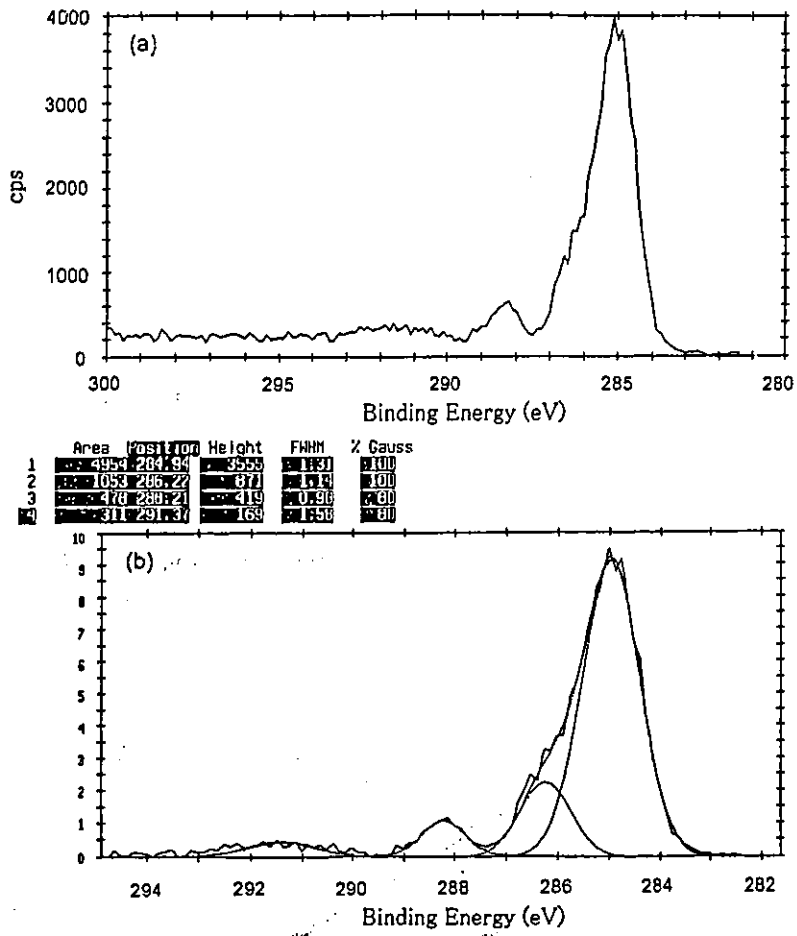

図 4.2 XPS スペクトルとピーク分類
(a) 取得スペクトル
(b) ピーク分離計算結果と分離ピークの表示

1）このスペクトル図は横軸の範囲が 280～295eV を描いていることから，測定している元素は炭素原子であることがわかる。
2）この材料の表面には少なくとも 3 種類の結合様式の炭素原子が存在する。
3）そのうち一種は C-C もしくは C-H で，あとの 2 つは酸素原子か窒素原子に結合している。
4）3 種のうちでは C-C もしくは C-H が最も多い。

このように ESCA のスペクトルからは元素と，さらにその結合様式の比を知ることができる。以下に，それぞれの点について説明する。

4.3 ESCA 測定の実際

4.3.1 サンプルの準備

正確でノイズの少ない ESCA スペクトルを得るための第一条件は高い真空度を保つことである。一般に，高分子材料の測定は敬遠される場合が多い。これは高分子材料が気体を収着しているため真空度が上がりにくい（占有時間が長くなる），軟 X 線照射によって試料から分解ガスが放出され，内部が有機物で汚染される，などのためである。しばしば試料の固定に用いられる両面テープも，ガスが出やすいので，試料の固定には，ねじ止めのホルダーを準備したほうがよい。試料に溶存しているガス・水分を減らすためには，前日から真空下で保存し直前に窒素ガスで置換してから試料室に導入する。

測定試料の形態も重要である。ESCA では平面性が測定データに影響する。後述する Depth Profile を測定する場合などは，理論上は完全に平滑な表面が要求される。実際にも走査型電子顕微鏡で鏡面にみえる程度の試料が必要である。凹凸の大きな試料，繊維，微粒子などの複雑な形状の試料を測定したい場合には，試料が散逸しないようにしっかりと試料台に固定し，得られたデータは平滑な表面で測定した場合と異なっている可能性があることに注意する必要がある。

4.3.2 測定条件

高分子材料を測定する場合にはスキャン条件を材料に合わせた設定にすること。具体的には 1 ステップあたりの測定時間，使用するスリットに注意する。有機材料と金属材料では放出される電子が極端に違うので，特に有機材料を測定する場合には高い S/N 比が得られるように設定する。またアルゴンイオンエッチング，繰り返しスキャンについては十分検討してから実施する。これらの手法はそれぞれ表面汚染層の除去および S/N 比の向上に有効であるが，いずれもエネルギーを表面に与えるので化学反応や蒸散などが起こることがある。

また測定データは制御用のコンピュータに保存されるが，これらのデータを利用するために VAMAS

(Versailles Project on Advanced Materials and Standards) 形式[8]で保存すれば，以下に述べるピーク面積計算やピーク分離がパソコンで実施できる。

4.3.3 ESCA スペクトルの解析

a）チャージのキャンセル

高分子材料は多くは絶縁体のため，測定中に電荷を帯びることがある。チャージアップといわれスペクトル全体が高エネルギー側にシフトした形で現れる。これをキャンセルするためにC1sを基準スペクトルとして285.0eVに設定し，スペクトル全体を修正する。

b）元素比の求め方

まず用いる装置で測定可能なエネルギー範囲を大まかにスキャンし，表面に存在する元素を確認する（ワイドスキャン：図4.3参照)。それぞれの元素のピーク位置は文献的に既知であるので，ピーク位置から表面に存在する元素の種類を把握することができる。その後，各元素のピーク位置周辺を分解能（ステップ数）をあげて再スキャンする。分子構造がわかっている場合には目的の元素に絞ってスキャンするが，ESCAは高感度なので，予期せぬコンタミネーションでデータが台無しになることを避けるためにワイドスキャンの測定を推奨する。元素ごとのスペクトルが得られたら，それぞれの全ピーク面積を測定し，元素間での面積比を求める。その際，それぞれのピーク面積を規格化する必要がある。

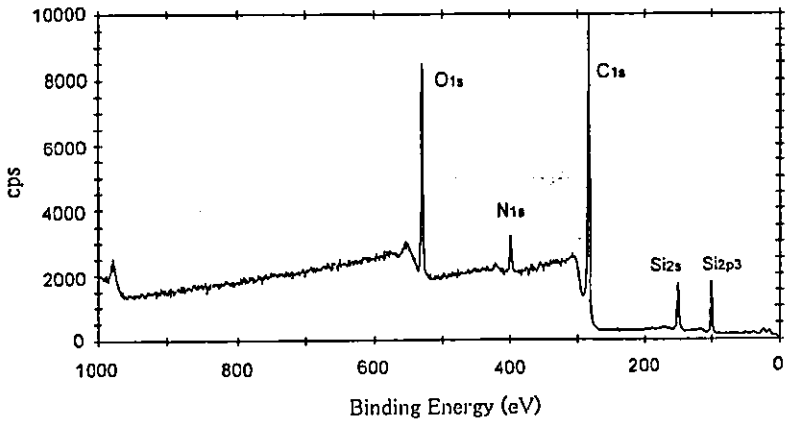

図4.3 シリコーン含有高分子のXPSワイドスキャン

規格化とは，C1sスペクトルの単位分子あたりのcpsの値を1とし，他の元素について比較することを指す。例えばC1sのピーク面積が10,000，O1sのピーク面積が20,000のとき，単純にCとOの比を1:2とはできない。C1sの相対強度を1としたとき，O1s酸素の相対強度は2.9である。すなわち一つの酸素原子から放出されるO1s電子の数はC1s電子の2.9倍ということである。そこで，この場合CとOの存在比は10000/1：20000/2.9≒10000：6900となる。すでにC1sの相対強度を1とした場合の他の元素の相対強度が求められているので，それらの数値を用いて面積比を計算する。ただし装置によっては文献の相対強度とは一致しない場合もある。できれば種々の高分子材料のESCA測定を行い，装置の傾向をつかんでおいた方がよい。例えばポリテトラフルオロエチレン，ポリメチルメタクリレート，ポリスチレンおよびポリエチレンなどを用い，測定のたびにリファレンス物質として同時に測定しておけば，それらのスペクトルを常に比較することで，装置の真空度や材料による汚染などをチェックすることができる。

c）ピーク分離

得られたスペクトルが図4.2 (a)のように複数のピークが含まれている場合，ピーク分離を行う。なぜ同じ元素で複数のピークが得られるのかは以下の理由による。電子の結合エネルギーは，元素がどのような結合をしているかによって異なる。例えばC-H結合のC1s軌道のエネルギーとC＝O結合の炭素の1s軌道の電子のエネルギーでは後者の方が高い。この差を化学シフトと呼ぶ。これらはすでにデータベース化されており，ピークを分離する際の目安となる。ピーク分離は装置を制御しているコンピュータ（大概はUNIX）で行うが，マシンタイムが混んでいたり，いろいろな分離法を試すときにはデータを持ち帰り，パソコン上で処理することもできる。ピークを分離する際に注意することは，

① やみくもに数字を追わない：ピーク分離の計算はソフトウエア上で行うものであるが，時として数字あわせに終始して現実とかけ離れた数値を出すことがある。例えば，ピークの分離にはベースラインを引き，ピークの形状を表す関数を選択し，

半値幅（ピーク高さの中点におけるピーク幅），非対象性パラメータなどの数値を入力して，計算を行って計算値を実測値にフィッティングさせてゆく。この際，それぞれのパラメータは自由に変更できるため，あり得ない数値を用いて計算上でピーク分離をしてしまうことがある。特に半値幅を小さくしたり，ピーク数を増やしたりすると，高い精度で分離できた結果が得られることがある。

② リファレンスと比較する：化学シフトの数値については，報告されているので，これと比較すること。ただし，研究者によって報告にばらつきがあるので，一つの数値に固執しないで，ある程度の幅があることを認識すること。

③ 精度について認識すること：ピーク分離のためにはS/N比の高いスペクトルデータが必要である。そのためには先に挙げたように，高真空度・汚染のないことなどが満たされている必要がある。得られたスペクトルがブロードでcps値も高くない場合に行ったピーク分離結果は相当の誤差を含んでいる。図4.2 (b) に (a) のスペクトルのピーク分離後の一例を示した。左上の数値はピーク分離後の計算値である。左からピーク面積，ピーク位置，cpsの値，半値幅，分離に用いた関数系中のガウス関数の分率が示されている。288.21 eVのピークの半値幅が小さすぎることがわかる。ベースラインの設定を含めて再計算の検討が必要と判断される。また，ピーク分離後にそれぞれの成分（例えばC−OとC=Oなど）の比をもとめ，分子構造を推定することもできる。

正確なピーク分離は多様な情報を与える。恣意的な分離はデータの捏造と同じである。できれば経験のある第3者に分析対象物質を告げずにピーク分離を行ってもらい，客観性のあるデータを得るべきである。

d）Depth Profiling

ESCAは材料表面の分析であるが，分析できる深さは高分子材料で数十Åである。通常得られる情報は，この深さの間の元素の平均化されたものである。深さ方向によって不均一であるかどうかは，このままでは知ることができない。この数十Å以内の深さ方向の分析を行おうとするのがDepth Profilingと呼ばれる方法である。

Depth Profilingにはいろいろな方法が考案されているが，以下に示す角度変化法がもっとも簡便であり，多用されている。図4.4に示すように試料平面の法線と装置のスリットが角度90度をなす場合が通常の状態である。試料をスリットに対して傾けると，検出器に入射する電子は，スリットに垂直に入射する方向に放出される必要がある。また電子が材料中を通過できる距離は決まっているので，脱出深度の距離を通過して表面から出る必要がある。このとき，電子が放出された位置にある原子の深さは90度の場合の$\sin\theta$倍になり，浅くなっている。すなわち試料の傾きを大きくすると，より表面外層部分のデータが得られるため，傾きを変化させて測定することで深さ方向の情報が得られるわけである。得られたデータは横軸に$\cos\theta$，縦軸にそれぞれの元素比や官能基比をとることで，視覚的に深さ方向の情報を得ることができる。

凹凸のある試料，繊維，微粒子を測定する場合に注意を要すると先に指摘したが，これは試料が平滑

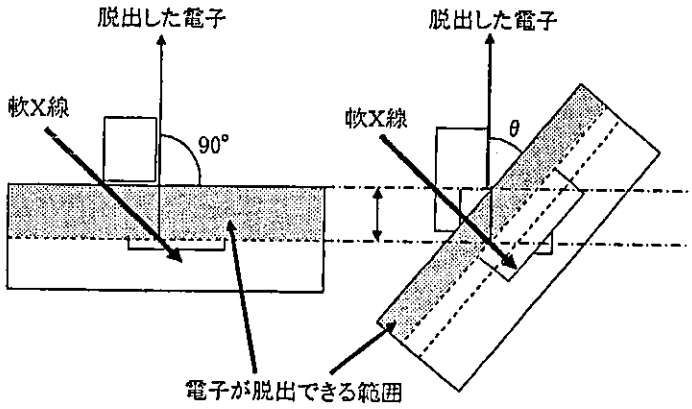

図4.4 試料角度による検出深さの変化

でない場合，測定深度がまちまちになり表面最外層の情報が強調されがちになるためである。この点を理解してデータを考察する必要がある。

4.4 データ解析における注意点

ESCAのデータ解析において重要な点は，絶対値ではなく，すべて相対値で比較する必要があることである。例えばO 1sのピーク面積の大小で酸素の存在量の大小は論じられない。C 1sスペクトルとの面積比で示す必要がある。また炭素や酸素の汚染源は

他にもあり，それらによって正しいスペクトルが得られていないことがある。このような事態を避けるために元素比とスペクトルの形状を合わせて考察を行う必要がある。

またピーク分離プログラムの計算結果に頼らず，それぞれのパラメータを吟味し裏付けをとる必要がある。例えばスペクトルのピーク分離の際に，個々のピークの半値幅を変化させて計算を行うが，半値幅の変化量には限度がある。解析ソフトウエアで設定できる自由度が高くなるほど恣意的になる危険性があるので注意が必要である。

4.5 接着と ESCA

ESCA は接着の現象を研究する上で強力な手段である。例えば，接着面の官能基の存在・種類を知ることができる。これによって，適切な接着剤の選択に有用な情報が得られる。また接着面を測定することによって，表面汚染層の確認も可能である。剥離面を測定すれば，界面破壊あるいは凝集破壊のメカニズムについての知見を得ることができる。接着面が高分子材料でも，金属あるいは無機材料でも同様である。

おわりに

以上，ESCA の測定からデータ解析までを概説した。化学修飾による官能基の分析や定量化の試み，最新の ESCA については文献を参考にしていただきたい[10～13]。分解能が向上し，マッピングも可能になるなど ESCA は進歩を続けているが，重要な点はスペクトルの意味をきちんと理解することである。ESCA は非常に有用な装置であり，正しく解析を行い解析に役立てていただきたい。

文 献

1) D. Briggs, M.P. Seah, eds. "Practical Surface Analysis-Vol.1 Electron Spectroscopy", John Wiley & Sons, New York (1992).
2) 筏 義人編, "高分子表面の基礎と応用 (上)", 化学同人, (1986).
3) 日本化学会編,"化学総説, No.16, 電子分光", 学会出版センター, (1977).
4) G. Beamson, D. Briggs, "High Resolution XPS of Organic Polymers, The Scienta ESCA300 Database", John Wiley & Sons, New York (1992).
5) 石谷 炯, "繊維・高分子測定法の技術", 繊維学会編, p.173 ,朝倉書店, (1985).
6) K.M. Shakesheff, M.C. Davies, R.L.Langer, Surfactant Sci. Ser., 87, 143 (1999).
7) N.H. Turner, J.A. Schreifels, Anal. Chem., 72, 99R (2000).
8) 森河 務, http://www.tri.pref.osaka.jp/group/surface/Esca/
9) M.P. Seah, M.T. Brown, J. Electron Spectrosc. Relat. Phenom., 95, 71 (1998).
10) J.E. Fulghum, J. Electron Spectrosc. Relat. Phenom., 100, 331 (1999).
11) V.I. Povstugar, S.S. Mikhailova, A.A. Shakov, J. Anal. Chem., 55, 405 (2000).
12) 河合 潤, ふぇらむ, 5, 298 (2000).
13) 松林信行, 触媒, 42, 277 (2000).

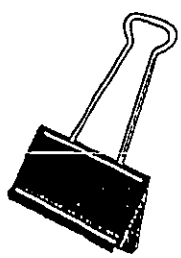

nd, at least partially, prevented the pulmonary vascular emodelling that occurs in this model. Although not conlusive, this study suggests that deficiency of H_2S might ontribute to the pathology (pulmonary vasoconstriction nd intimal thickening) of this disease.

The possibility that excess H_2S contributes to the ypotension that is associated with either septic (caecal igation and puncture) or endotoxic shock in the rat as also been raised [13]. In this work, H_2S concentrations homogenates prepared from the aorta, pulmonary, esenteric and tail arteries were significantly increased hen compared with controls, which suggests that overroduction of this vasodilator gas can play a part in the ascular consequences of both disease states.

Although these new data provide preliminary evidence or a role of H_2S in vascular disease many questions emain to be answered. For example, it is not clear hether the changes in H_2S levels recently observed in iimals with experimental models of cardiovascular isease are a cause or a consequence of the disease. lthough inhibitors of H_2S synthesis such as DL-propar-lglycine (CSE inhibitor) and aminooxyacetic acid (CBS nhibitor) have been described, both inhibit other enzymes id as such might have additional effects. Thus, potent nd selective CSE and CBS inhibitors are now required. he availability of such compounds should facilitate the dentification of the biological significance of H_2S.

Finally, it should be noted that NO, CO and H_2S might ot be the only biologically active gases of interest to the harmacologist. Ammonia, found in large amounts in the ody, has vasoconstrictor activity perhaps by intracellular alkalinization [14]. Sulfur dioxide (SO_2) and nitrous oxide (N_2O) are products of bacterial metabolism and also exhibit pharmacological effects in animals. For example, SO_2 is a vasodepressor in the rat [15] and increases neutrophil adhesion to cultured pulmonary epithelial cells [16] whereas N_2O inhibits glutamate-mediated transmission possibly by acting as an NMDA receptor antagonist [17]. Gases have a special advantage as biologically active mediators because they are able to infiltrate the three-dimensional structure of receptors, enzymes and channels and alter their chemical structure so as to affect function.

References

1 Wang, R. (2002) Two's company, three's a crowd: can H_2S be the third endogenous gaseous transmitter? *FASEB J.* 16, 1792–1798
2 Kimura, H. (2002) Hydrogen sulfide as a neuromodulator. *Mol. Neurobiol.* 26, 13–19
3 Eto, K. *et al.* (2002) Hydrogen sulfide is produced in response to neuronal excitation. *J. Neurosci.* 22, 3386–3391
4 Eto, K. and Kimura, H. (2002) The production of hydrogen sulfide is regulated by testosterone and S-adenosyl-L-methionine in mouse brain. *J. Neurochem.* 83, 80–86
5 Zhao, W. *et al.* (2001) The vasorelaxant effect of H_2S as a novel endogenous gaseous K(ATP) channel opener. *EMBO J.* 20, 6008–6016
6 Eto, K. and Kimura, H. (2002) A novel enhancing mechanism for hydrogen sulfide-producing activity of cystathionine β-synthase. *J. Biol. Chem.* 277, 42680–42685
7 Silva, A.J. (2003) Molecular and cellular cognitive studies of the role of synaptic plasticity in memory. *J. Neurobiol.* 54, 224–237
8 Sattler, R. and Tymianski, M. (2001) Molecular mechanisms of glutamate receptor-mediated excitotoxic neuronal cell death. *Mol. Neurobiol.* 24, 107–129
9 Eto, K. *et al.* (2002) Brain hydrogen sulfide is severely decreased in Alzheimer's disease. *Biochem. Biophys. Res. Commun.* 293, 1485–1488
10 Kamoun, P. *et al.* (2003) Endogenous hydrogen sulfide overproduction in Down syndrome. *Am. J. Med. Genet.* 116A, 310–311
11 Teague, B. *et al.* (2002) The smooth muscle relaxant effect of hydrogen sulphide *in vitro*: evidence for a physiological role to control intestinal contractility. *Br. J. Pharmacol.* 137, 139–145
12 Chunyu, Z. *et al.* (2003) The regulatory effect of hydrogen sulfide on hypoxic pulmonary hypertension in rats. *Biochem. Biophys. Res. Commun.* 302, 810–816
13 Hui, Y. *et al.* (2003) Changes in arterial hydrogen sulfide (H_2S) content during septic shock and endotoxin shock in rats. *J. Infect.* 47, 155–160
14 Krampetz, I.K. and Rhoades, R.A. (1991) Intracellular pH; effect on pulmonary arterial smooth muscle. *Am. J. Physiol.* 260, L516–L521
15 Meng, Z. *et al.* (2003) Blood pressure of rats lowered by sulfur dioxide and its derivatives. *Inhal. Toxicol.* 15, 951–959
16 Pelletier, M. *et al.* (2002) Activation of human epithelial lung a549 cells by the pollutant sodium sulfite, enhancement of neutrophil adhesion. *Toxicol. Sci.* 69, 210–216
17 Balon, N. *et al.* (2003) Nitrous oxide reverses the increase in striatal dopamine release produced by N-methyl-D-aspartate infusion in the substantia nigra pars compacta in rats. *Neurosci. Lett.* 343, 147–149

doi:10.1016/j.tips.2003.10.007

A site-specific polymeric drug carrier for renal disease treatment

Akio Kishida

Department of Biomedical Engineering, National Cardiovascular Center Research Institute, 5-7-1 Fujishiro-dai, Suita, Osaka 565-8565, Japan

A well-designed polymeric carrier for site-specific drug delivery in the treatment of renal disease has been reported recently. Approximately 80% of the water-soluble polymer poly(vinylpyrrolidone-co-dimethyl maleic anhydride selectively accumulated in the kidney of mice 24 h after intravenous injection. The detailed mechanism of such selective accumulation is not clear but an energy-dependent process, other than endocytosis, might be involved in the uptake of the polymer. This study is the first to report active targeting using a synthetic polymeric drug carrier.

A variety of both natural and synthetic water-soluble polymers have been used for medical, surgical and

Corresponding author: Akio Kishida (kishida@ri.ncvc.go.jp).

pharmaceutical applications. The field in which these polymers have been applied most frequently is pharmaceutics because they are believed to be effective in the controlled release of drugs. Conventional dosage forms are not always sufficiently effective at targeting drugs to their site of action and in releasing active agents over a desired period of time and thus novel and innovative drug delivery systems are being studied to solve this problem.

Polymeric carriers

To develop a new polymeric carrier for a given drug, an analysis of the distribution of polymers within the body is important because this directly affects drug efficacy. There are at least two strategies that could be used to control the body distribution of water-soluble drugs: active and passive targeting. In the former strategy, the drug is delivered to target cells or tissues by means of a homing moiety such as monoclonal antibodies that are specific to tumor cell-surface antigens [1–4]. This approach seems to be very efficient at targeting the drug to tumor tissue; however, the homing moiety itself might be immunogenic. By contrast, passive targeting is not associated with immunogenicity or toxicity if bio-inert polymers are used as drug carriers. Passive targeting of drugs using such polymeric carriers can increase the efficacy of the drug because: (i) the half-life of the drug in the circulation is prolonged as a result of the increased size of the drug–carrier complex; (ii) vascular permeability is higher at the site of injury compared with unaffected areas; and (iii) the carrier polymer interacts with body components. These factors should enhance the bioavailability of the drug, reduce the dose of drug required and minimize the side-effects of the drug. Because the biological fate of drugs bound to carrier matrices is generally determined by that of the carrier itself, it is important to accumulate detailed information on the body distribution or the biological fate of drug carriers [5,6].

A new water-soluble polymer

The application of a novel drug carrier, the water-soluble polymer poly(vinylpyrrolidone-co-dimethyl maleic anhydride) [poly(VP-co-DMMAn)], to the treatment of renal disease was reported recently [7]. A commonly encountered problem in pharmacokinetic studies of the body distribution of polymers is the differential dispersal of polymers with different molecular weights, particularly while the polymer is in the circulation. To avoid this problem, Tsutsumi and colleagues purified the poly(VP-co-DMMAn) polymer using gel filtration chromatography to obtain polymers with a narrow molecular weight distribution (polydispersity [Mw/Mn] = 1.04) [7]. Both vinylpyrrolidone and dimethyl maleic anhydride are common monomers for preparing such biomaterials and thus the toxicity and biological activity of these polymers have been widely studied and the polymerization kinetics of the co-polymer are controllable. The optimum composition of the co-polymer for renal drug delivery was obtained at high yield and good reproducibility. Approximately 80% of the dose of the polymer selectively accumulated in the kidney of mice 24 h after intravenous injection. The detailed mechanism of this distribution is not clear but the efficacy and non-toxicity of the polymer was sufficient such that Tsutsumi and colleagues believe it can be used successfully as a drug carrier.

Why dose the polymer accumulate in the kidney?

It is well known that the molecular weight and electric charge of polymers influence their distribution to organs such as the kidney, lung and liver. Generally, the urinary clearance of polymers decreases with increasing molecular weight. The vascular wall of glomeruli functions as a filter of substances in the kidney based on their molecular size and electric charge [8,9]. The cut-off molecular weight of globular proteins for glomerular permeability is reported to be ~60 000 [8]. The molecular weight of the polymer that Tsutsumi and colleagues prepared was ~10 000 and the electric charge was negative as a result of the hydrolyzed dimethyl maleic anhydride position. It has been reported that negative charge reduces the glomerular filtration of polymers because of the electrostatic repulsion between the negative charge of the vascular wall and the anionized polymer [9]. In the study by Tsutsumi and colleagues, poly(VP-co-DMMAn) was eliminated quickly from the circulating blood but was not excreted from the kidney, and accumulated in the cortex and renal tubules. This result suggests that an active process of poly(VP-co-DMMAn) uptake exists. Definitive identification of such a process would represent a breakthrough in the development a new frontier of site-specific (targeting) drug delivery systems using specific polymers.

How does poly(VP-co-DMMAn) compare with poly(ethylene glycol)?

Among the various polymeric carriers, the most widely used is poly(ethylene glycol) (PEG). Various proteins and drugs have been modified by PEG to enhance their therapeutic efficacies [10–16]. These studies demonstrated that PEG modification was effective in: (i) prolonging the half-life of drugs in the circulation; (ii) changing the body distribution of drugs; (iii) protecting the drugs from 'attack' by proteases and antibodies; and (iv) reducing the antigenicity of drugs. Therefore, it is believed that PEG conjugation to protein drugs is a useful strategy to modify the pattern of drug distribution for improved therapeutic efficacy and reduced side-effects of drugs.

Poly(VP-co-DMMAn) possesses reactive functional groups and accumulates specifically in the kidney. However, sometimes such functional chemical groups can give rise to difficulties. For example, multivalent reactive groups of polymers make it difficult to characterize the conjugate. Although there are problems associated with these polymers, Tsutsumi *et al.* have demonstrated the treatment of acute renal failure using poly(VP-co-DMMAn)–superoxide dismutase (SOD) [PVDn–SOD]. Indeed, PVDn–SOD accumulated effectively in the kidney and produced a notable therapeutic effect at a reasonable dose.

Polymers in pharmacy and drug delivery systems

Various kinds of polymers that include functional groups have been reported [15,16] and some are undergoing clinical trials or are already in clinical use for drug delivery [17,18]. Tsutsumi and colleagues have also reported the

use of protein drugs conjugated with PEG [19,20]. In these studies, they purified the polymer until the polymer had a single molecular weight. It is necessary to use the purified polymer to evaluate the tissue distribution of the polymer scientifically and quantitatively. Many experiments and physical analyses of these polymer chains in solution are necessary to determine whether Tsutsumi and colleagues' method of preparing polymeric drug carriers can be used generally for site-specific drug delivery. However, the study by Tsutsumi and colleagues has paved the way for developing such a technique.

References

1 Brich, Z. *et al.* (1992) Preparation and characterization of a water soluble dextran immunoconjugate of doxorubicin and the monoclonal antibody. *J. Control. Release* 19, 245–258
2 Igarashi, R. *et al.* (1992) A stable PGE_1 prodrug for targeting therapy. *J. Control. Release* 20, 37–46
3 Kopecek, J. (1991) Targetable polymeric anticancer drugs. Temporal control of drug activity. *Ann. New York Acad. Sci.* 618, 335–344
4 Nishikawa, M. *et al.* (1992) Pharmacokinetics of receptor-mediated hepatic uptake of glycosylated albumin in mice. *Int. J. Pharm.* 85, 75–85
5 Yamaoka, T. *et al.* (1995) Fate of water-soluble polymers administered via different routes. *J. Pharm. Sci.* 84, 349–354
6 Yamaoka, T. *et al.* (1994) Distribution and tissue uptake of poly (ethylene glycol) with different molecular weights after intravenous administration to mice. *J. Pharm. Sci.* 83, 601–606
7 Kamada, H. *et al.* (2003) Synthesis of a poly(vinylpyrrolidone-co-dimethyl maleic anhydride) co-polymer and its application for renal drug targeting. *Nat. Biotechnol.* 21, 399–404
8 Brenner, B.M. *et al.* (1978) Glomerular permselectivity: barrier function based on discrimination of molecular size and charge. *Am. J. Physiol.* 234, F455–F460
9 Takakura, Y. *et al.* (1990) Disposition characteristics of macromolecules in tumor-bearing mice. *Pharm. Res.* 7, 339–346
10 Veronese, F.M. *et al.* (2002) Polyethylene glycol-superoxide dismutase, a conjugate in search of exploitation. *Adv. Drug Deliv. Rev.* 54, 587–606
11 Hinds, K.D. and Kim, S.W. (2002) Effects of PEG conjugation on insulin properties. *Adv. Drug Deliv. Rev.* 54, 505–530
12 Kozlowski, A. *et al.* (2001) Development of pegylated interferons for the treatment of chronic hepatitis C. *BioDrugs* 15, 419–429
13 Duncan, R. and Spreafico, F. (1994) Polymer conjugates. Pharmacokinetic considerations for design and development. *Clin. Pharmacokinet.* 27, 290–306
14 Delgado, C. *et al.* (1992) The uses and properties of PEG-linked proteins. *Crit. Rev. Ther. Drug Carrier Syst.* 9, 249–304
15 Auzely-Velty, C. *et al.* (2002) Galactosylated N-vinylpyrrolidone-maleic acid copolymers: synthesis, characterization, and interaction with lectins. *Biomacromolecules* 3, 998–1005
16 Murthy, N. *et al.* (2003) Design and synthesis of pH-responsive polymeric carriers that target uptake and enhance the intracellular delivery of oligonucleotides. *J. Control. Release* 89, 365–374
17 Pedder, S.C. (2003) Pegylation of interferon alfa: structural and pharmacokinetic properties. *Semin. Liver Dis.* 23 (Suppl. 1), 19–22
18 Milas, L. *et al.* (2003) Poly(L-glutamic acid)-pacritaxel conjugate is a potent enhancer of tumor radiocurability. *Int. J. Radiat. Oncol. Biol. Phys.* 55, 707–712
19 Tsutsumi, Y. *et al.* (1994) Chemical modification of natural human tumor necrosis factor-alpha with polyethylene glycol increases its antitumor potency. *Jpn. J. Cancer Res.* 85, 9–12
20 Yamamoto, Y. *et al.* (2003) Site-specific PEGylation of a lysine-deficient TNF-alpha with full bioactivity. *Nat. Biotechnol.* 21, 546–552

0165-6147/$ - see front matter
doi:10.1016/j.tips.2003.10.009

Interleukin 4 treatment of psoriasis: are pleiotropic cytokines suitable therapies for autoimmune diseases?

Roland Martin

Cellular Immunology Section, Neuroimmunology Branch, National Institute of Neurological Disorders and Stroke, National Institutes of Health, 10 Center DR MSC 1400, Bethesda, MD 20892-1400, USA

Many human autoimmune diseases are still treated by a combination of corticosteroids and general immunosuppression. A better understanding of the pathogenesis of these diseases has led to therapies that are more specific than current therapies of some of these disorders. In psoriasis, T helper (Th) cells with a pro-inflammatory phenotype (Th1) are considered essential to the disease process. A recent clinical trial of interleukin 4 in psoriasis has demonstrated that such pleiotropic cytokines can be used safely and effectively to correct imbalances in immune function.

In many respects, psoriasis is a typical autoimmune disease [1]. Psoriasis affects a specific organ, the skin, and, to a lesser extent, joints, tendons and ligaments. Inflammatory infiltrates, tissue destruction, clinical heterogeneity and a complex genetic background are all characteristics of psoriasis, type 1 diabetes, rheumatoid arthritis (RA), multiple sclerosis (MS) and other autoimmune diseases. Approximately 2% of the population suffer from papules, nodules and thickened, scaly plaques that appear in distinct areas of the body, such as the elbows and knees, or affect large areas of the skin. When the disease is more widespread and joints become involved, psoriasis can severely compromise the quality of life of the patient and has a substantial socioeconomic impact [2].

The cause of psoriasis is unknown but a combination of genetic predisposition and environmental factors probably triggers the autoimmune process. Pathogenetically, psoriasis is characterized by oligoclonal T-cell infiltrations, which accompany other immune cells such as monocytes, and a chronic change in tissue turnover and architecture

Corresponding author: Roland Martin (martinr@ninds.nih.gov).

心臓弁の凍結保存

庭屋　和夫，北村惣一郎

国立循環器病センター　心臓血管外科

Cryopreservation of homograft heart valve.

Kazuo Niwaya, M.D. and Soichiro Kitamura, M.D.

Cardiovasular Surgery, National Cardiovascular Center, Osaka, Japan

1．同種心臓弁の変遷

現在，心臓弁置換手術に用いられる代用弁は，主にブタ大動脈弁ないしはウシ心膜をグルタルアルデヒド処理した「異種生体弁」か，パイロライトカーボン製の弁葉を持つ，いわゆる「機械弁」が臨床使用されている。両者それぞれに，耐久性，抗血栓性，代用弁感染などの点で利点とともに問題点を併せ持ち，症例の背景に応じて代用弁の選択がされている。一方，諸外国ではこれらの選択枝に加えて凍結保存同種弁（ホモグラフト弁）が大動脈弁位あるいは肺動脈弁位に使用されてきた。歴史的には，現在汎用されている代用弁が臨床使用されるようになる以前の1956年に，Murrayが大動脈閉鎖不全症の患者の胸部下行大動脈に新鮮ホモグラフト弁を移植した[1]。それに引き続き1962年にRoss[2]，次いでBarratt-Boyesら[3]がそれぞれ，新鮮ホモグラフト弁による同所性大動脈弁置換術の成功を報告した。当時は，心停止後のドナーからホモグラフト弁を採取した後，短期間（数日）の冷蔵保存の後，臨床使用していた。その後入手困難なホモグラフト弁の保存期間の延長と有効な滅菌を目的として，β-プロピオラクトン処理などの化学的処理や放射線処理が導入されたが，それらの処理を行ったホモグラフト弁は臨床成績が芳しくないことが明らかになり，その後同様の処理方法は継続されることはなかった。一方，抗生物質を加えた液体栄養培地で数週間冷蔵保存したホモグラフト弁（fresh-wet stored homograft）を用いた大動脈弁置換術の成績は，再手術回避率，血栓塞栓症回避率とも他の代用弁と比較しても満足できる成績で，ホモグラフト弁の有用性の認識は維持された。1973年，Angellら[4]により報告された方法を発展させ，O'Brienら[5]はホモグラフト弁を採取後短期間抗生物質で滅菌処理した後，細胞凍結障害防止剤と液体栄養培地を使用しプログラムフリーザーで緩徐凍結する方法（cryopreservation）を導入した。彼らが報告した凍結保存ホモグラフト弁による大動脈弁置換術は，術後15年での血栓塞栓症回避率が95%，心事故回避率が80%と良好な成績を示した。凍結保存法の導入により，移植用組織を取り扱うtissue bankが整備されることとなり，凍結保存ホモグラフト弁が比較的容易に入手できる環境が出来たことも重なり，結果，人工弁が種々の進歩を遂げた現在でも，ホモグラフト弁は代用弁の貴重なひとつの選択肢とされている。

【キーワード】
同種弁，凍結保存，cryopreservation，tissue engineering valve，組織バンク

2．ホモグラフト弁の凍結保存方法

ホモグラフト弁の摘出手技に関しては，既に詳

別刷請求先：庭屋和夫　〒565-8565　大阪府吹田市藤白台5丁目7番1号 国立循環器病センター心臓血管外科